

RESEARCH PAPERS

Vegetative incompatibility and potential involvement of a mycovirus in the Italian population of *Geosmithia morbida*

LUCIO MONTECCHIO¹, GENNY FANCHIN¹, VALERIA BERTON² and LINDA SCATTOLIN¹

¹ Department Territorio e Sistemi Agroforestali, viale dell'Università 16, I-35020 Legnaro PD, Italy

² Istituto Zooprofilattico Sperimentale delle Venezie, viale dell'Università 10, I-35020 Legnaro PD, Italy

Summary. Studies carried out during an Italian outbreak of the Thousand Cankers Disease of walnut, demonstrated that non-coalescing cankers on host plants, separated by equidistant uninfected zones, were associated with incompatible strains of *Geosmithia morbida*. Confirmation of the vegetative incompatibility of paired fungal isolates, randomly collected from black walnuts, was obtained from observations of a clear separation zones and the absence of anastomoses. Pairing tests with two incompatible monoconidial strains indicated differences in morphology and growth rates. Electron microscopy revealed the presence of icosahedral mycovirus-like particles in one of the monoconidial strains that demonstrated low degrees of virulence *in planta* compared with a particle-free monoconidial strain. The occurrence of a vegetative incompatibility system in recently introduced populations of *G. morbida* has considerable implications for fungal biology. Incompatibility in *G. morbida* and potential direct or indirect roles of the observed virus-like particles have potential ecological and epidemiological consequences.

Key words: thousand cankers disease, walnut, *Juglans*, virulence.

Introduction

Thousand cankers disease (TCD) is a complex infection caused by the fungus *Geosmithia morbida* Kolařík (Ascomycota, Hypocreales) and its insect vector *Pityophthorus juglandis* Blackman 1928 (Coleoptera, Scolytinae; walnut twig beetle, WTB). Since the mid-1990s, the disease has been responsible for widespread mortality of Juglandaceae in the USA (Zerillo *et al.*, 2014), and more recently, the disease has caused tree mortality in Italy (Montecchio and Faccoli, 2014; Montecchio *et al.*, 2014).

Susceptible hosts are in the genera *Juglans* and *Pterocarya* (*J. ailantifolia*, *J. californica*, *J. cinerea*, *J. hindsii*, *J. major*, *J. mandshurica*, *J. microcarpa*, *J. mollis*, *J. nigra*, *J. regia*, *J. hindsii* × *J. regia*, *J. nigra* × *J. hindsii*, *J. cinerea* × *J. ailantifolia*, *J. nigra* × *J. regia*, *P. fraxinifolia*, *P. rhoifolia* and *P. stenoptera*; Wood and Bright, 1993;

Seybold *et al.*, 2012; Serdani *et al.*, 2013; Utley *et al.*, 2013). These host plants may occur naturally or be cultivated for fruit or timber, or as ornamental trees. The geographical distribution of susceptible species and hybrids frequently overlaps, and in combination with the natural dispersal of infected vectors and trade of infected wood commodities, this distribution explains the spread continuum of TCD over long distances. Susceptibility to TCD and symptom intensity vary among host species and hybrids (with *J. nigra* as the most susceptible species) and within species (Tisserat *et al.*, 2011; Freeland *et al.*, 2012; Utley *et al.*, 2013).

Macroscopic and non-specific symptoms of TCD can appear several years after infection, beginning as gradual yellowing, wilting and flagging of leaves followed by twig and branch death, and eventual tree death in the most susceptible genotypes. Affected trees die 3-5 years after appearance of the first symptoms (Tisserat *et al.*, 2009). Typical symptoms of TCD are also detectable in the early infection stages on

Corresponding author: L. Montecchio
E-mail: montecchio@unipd.it

twigs and branches, consisting of feeding wounds or entrance and exit holes produced by infected WTBs. These promote the fungal colonization of neighbouring subcortical tissues through the release of mycelial propagules or spores of *G. morbida*, which produce small subcortical cankers. Multiple infestations on individual branches and trees are typical because of compulsory feeding behaviour and reproductive strategies of WTB (Tisserat *et al.*, 2009; Zerillo *et al.*, 2014). These insects which produce multiple (often occurring every 2 to 5 cm) coalescing cankers that girdle branches, interrupt phloem functionality and result in the reported macroscopic symptoms. According to the available literature (e.g., Tisserat *et al.*, 2009; Zerillo *et al.*, 2014), the cankers are usually diffuse, dark brown to black, 10–20 cm, elongated lengthwise along host stems, and are coalesced.

Because the cankers are the only obvious aspect of TCD, disease surveys from the recently reported Italian outbreak took into account the canker locations, distribution and features. Apart from the common diffuse and coalescing cankers (Tisserat *et al.*, 2009), other types of cankers with previously unreported features were observed on black and European walnut trees, and a low percentage of cankers showed visible equidistant separation from the neighbouring lesions and frequently exhibited darker edges. Visibly non-coalescing cankers showed sub-parallel 2–3 mm wide separation lines, whereas partially coalescing cankers were separated by narrower and inconsistent whitish lines (Figure 1).

As multiple *G. morbida* haplotypes can be present on individual same trees (Zerillo *et al.*, 2014), these observations suggest that incompatible interactions occur between neighbouring isolates. Vegetative incompatibility among fungal genotypes of the same species is a known phenomenon (Glass and Demethon, 2006), that is involved in gene flow and ecology of a number of pathogenic Ascomycetes. This behaviour has practical consequences for fungal population dynamics and disease epidemiology (Brasier, 1988; Causin *et al.*, 1995; Brasier and Kirk, 2000; Cortesi and Milgroom, 1998; Liu and Milgroom, 2007; Brasier and Webber, 2013).

The study reported here was performed to investigate whether Italian isolates of *G. morbida*, which were probably introduced in recent years from the USA (Montecchio and Faccoli, 2014), exhibit vegetative compatibility and incompatibility reactions. Furthermore, the study aimed to determine if this di-

versity is associated with different degrees of pathogenicity and the presence of mycovirus, previously reported for other pathosystems (Anagnostakis, 1982; Polashock *et al.*, 1997; Zhou and Boland, 1997; Hong *et al.*, 1999; Deng *et al.*, 2003; Wu *et al.*, 2007; Rodriguez-Garcia *et al.*, 2014; Schoebel *et al.*, 2014).

Materials and methods

Preliminary vegetative compatibility tests on naturally infected black and European walnut trees

Samples were collected during the Italian TCD outbreak (Veneto Region; Bressanvido, VI, 45°39'N, 11°38'E) from 15- to 20-year-old infected black walnut trees.

Fifteen branches (4–8 cm diameter, and 80–120 cm long) with typical TCD necroses were collected from one symptomatic tree. After gentle removal of the outer bark, one branch showing three cankers close together, which probably originated from single WTB infections, was selected. Among them, two merging cankers (designated 1M and 2M) were partially separated by a very thin discontinuous line, while the third canker (designated U, unmerging) was visibly separated from 1M and 2M by a wide sub-parallel, apparently uninfected area (Figure 3a).

After surface treatment with 3% sodium hypochlorite, one 3 mm wide chip from the outermost edges of the three cankers was removed with a scalpel, placed on potato dextrose agar (PDA; BD Difco) and incubated at $27 \pm 1^\circ\text{C}$ in the dark (Kolarik *et al.*, 2011). After 7 d, amongst a variety of microorganisms, one fungal colony per canker with features matching both the available description (Kolarik *et al.*, 2011) and the local reference strain LM13GMN, which was previously isolated from *J. nigra* in the same geographic location (Montecchio and Faccoli, 2014), was sub-cultured to fresh PDA. Thus, three pure *G. morbida* isolates were obtained and coded according to the previous identification of the canker as 1M, 2M or U.

From each isolate, a 5 mm diameter plug was taken from the edge of a 10-d-old colony and transferred to PDA bottom-up and equidistant in a 9 cm diam. Petri dish. As a control, three plugs of the same isolate were plated together. Each treatment consisted of five replicates. Cultures were incubated at $27 \pm 1^\circ\text{C}$ in the dark.

Colony growth was evaluated visually for 90 d, examining the cultures for merging and classified as "PM" (partially merging: contact < 4 mm) or "U"

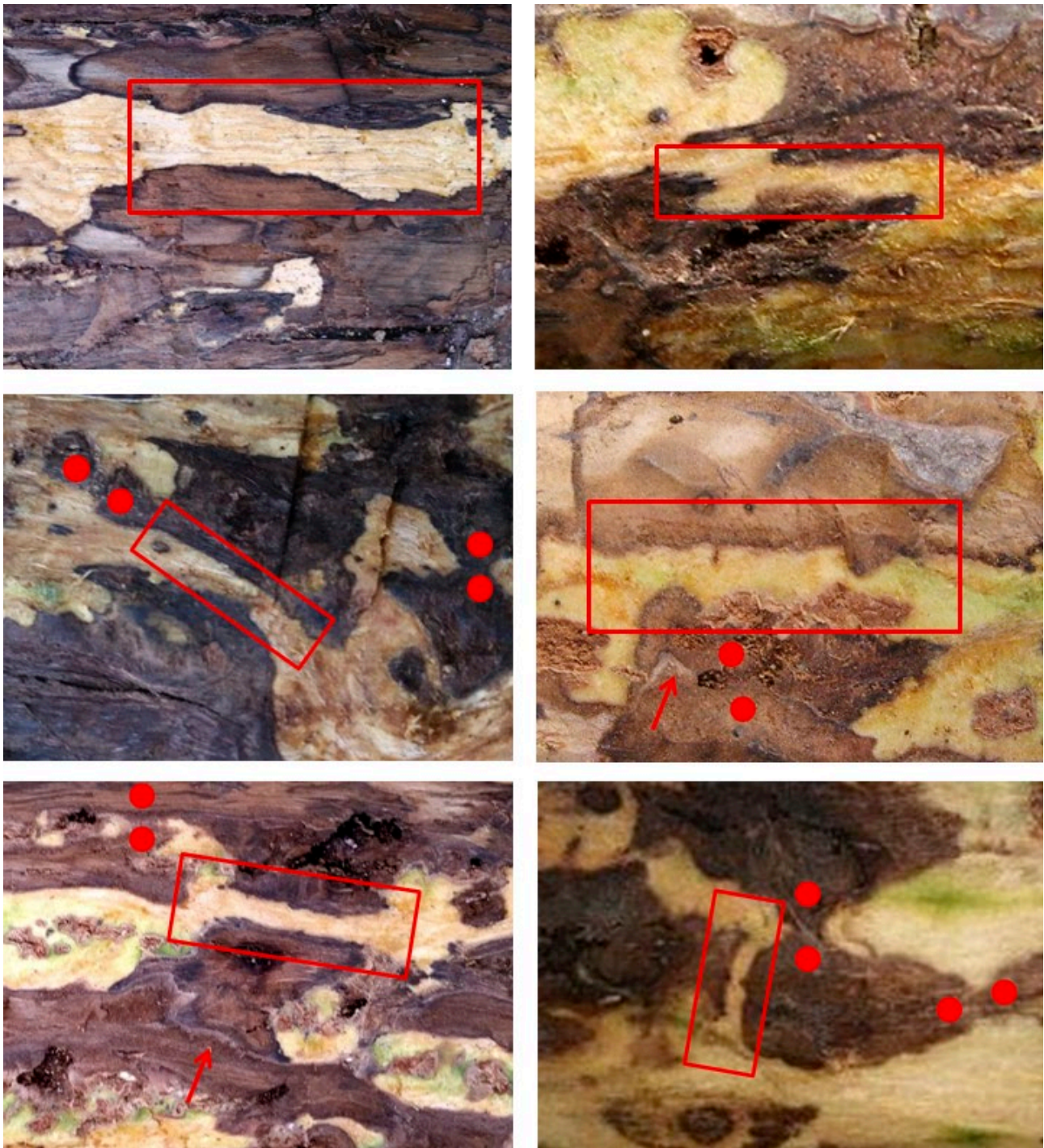


Figure 1. In addition to the typical diffuse and coalescing *Geosmithia morbida* cankers (facing dots), other cankers are separated by a constant sub-parallel line that is 2–3 mm wide and does not merge (rectangles) or by an inconstant thinner line (arrow) that partially merges. Left column: black walnut; right column: European walnut.

(unmerging; no contact), and compared with the classifications of the respective parental cankers.

Subsequently, all pairings that were closer than 5 mm were sectioned transversely at the point of closest vicinity, and the presence of hyphal anastomoses between mycelia investigated at 1000× magnification under a compound microscope.

Vegetative compatibility between isolates was subsequently classified as “LC” (likely compatible: partially merging, with uncertain presence of anastomoses) or “I” (incompatible: overlapping but not merging, without anastomoses).

Vegetative compatibility in the Italian outbreak

Isolate collection, macroscopic categorization and vegetative compatibility among isolates

Because TCD in European walnut trees has been reported in only four uneven-aged trees with unknown origin in only two localities, a detailed investigation was performed on black walnut to verify the vegetative compatibility among *G. morbida* strains obtained from single isolated cankers from the official Italian outbreak (Figure 2). Among the available potential sites, 12 comparable infected plantations were identified according to approximate tree

age (18 years) and likely genetic similarity as a result of originating from a single local nursery (“Cento vivaistico e per le attività fuori foresta”, Veneto Agricoltura, Regione del Veneto), which traditionally provides nut stocks from the same seed trees.

In 2014, one symptomatic tree per plantation was randomly selected, and one symptomatic branch portion (average diameter 4 cm, length 30 cm) was collected. One canker that was at least 6 cm from the closest neighbouring canker was then selected and treated as described above, to obtain one *G. morbida* isolate. The reference strain LM13GMN, coded as 1, was also added to the collection.

The 13 strains obtained were individually plated on PDA, incubated at $27 \pm 1^\circ\text{C}$ in the dark with 7 replicates, and after 21 d, categorized according to the following macroscopic features (Figure 4):

- 1) Pigmentation - “W” (whitish-orange) or “B” (orange-brown);
- 2) Edge shape - “E” (mainly even) or “R” (mainly rough);
- 3) Growth rate - “F” (fast, average diameter. measured along four opposite directions ≥ 3 cm) or “S” (slow, average diameter < 3 cm).

From the edge of one colony per strain, one 5 mm plug was transferred to PDA in a 14 cm diam.

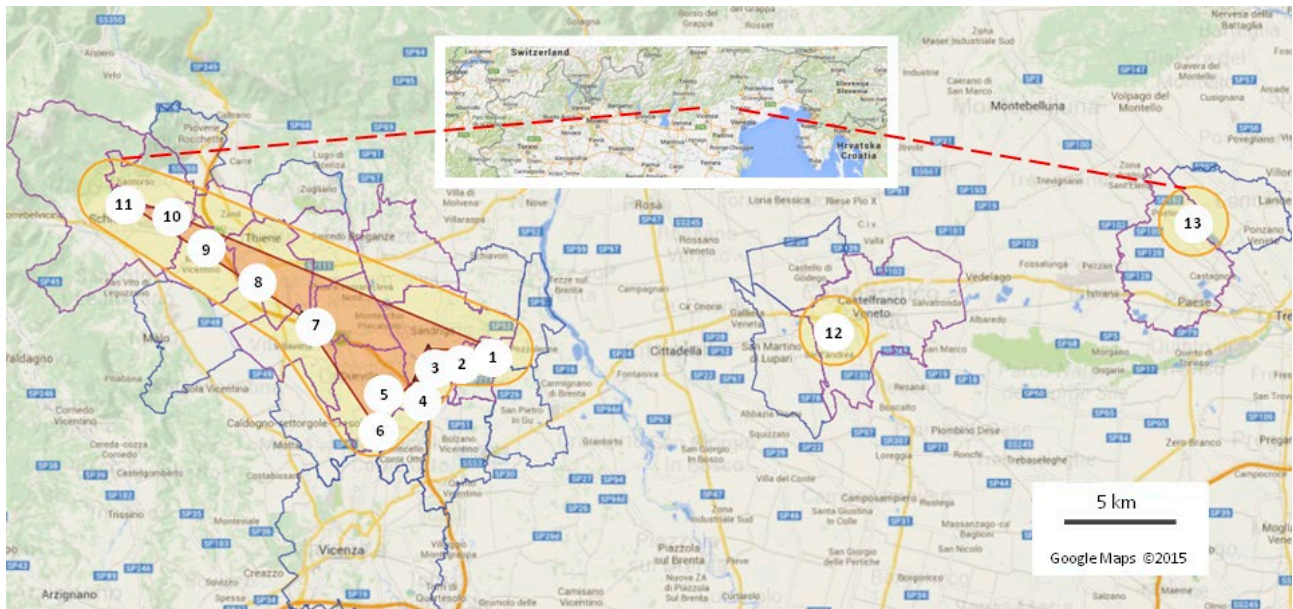


Figure 2. Official area of Italy affected by thousand cankers disease (pink) and buffer zone (yellow) as of August 2014 (Regione del Veneto, 2014). Sampling sites are numbered as reported in Table 1 (Cartographic basis: Google Maps 2015).

Petri dish, with 16 different plugs randomly placed bottom-up per dish in all possible combinations, on the intersections of a 3 cm grid, giving a total of 91 comparisons, including self-by-self pairings. The five empty spaces available in the last Petri dish were inoculated by randomly duplicating existing pairings. All cultures were prepared with seven replicates. The cultures were incubated at $27 \pm 1^\circ\text{C}$ in the dark. Colonies were examined every 3–4 d to compare growth with that of the previous day, which was temporarily delimited with a black line on the back of each Petri dish (Figure 4). At each observation time when growth was observed, the previous perimeter was removed and the new one marked. The trial finished when the slowest-growing colony failed to grow further for 15 d. Colony growth was evaluated visually, based on merging ability, which was classified as FM (fully merging), PM or U. All pairs closer than 5 mm were transverse sectioned at the point of closest vicinity, and the presence of hyphal anastomoses between mycelia investigated as reported above. Vegetative compatibility was then classified as C, LC or I.

In vitro vegetative compatibility between two diverging monoconidial strains

The W, E, and F isolates with the lowest I ratings amongst isolates with the highest C records were considered representative C isolates, and the B, R, and S isolates with the highest I ratings amongst those with the lowest C were considered representative I isolates. These were used to obtain monoconidial strains based on the methods of Causin *et al.* (1995).

From sub-cultures obtained from the isolates, a single monoconidial strain that confirmed all of the parental morphological features was selected and identified as “MC” (monoconidial compatible) and “MI” (monoconidial incompatible). Using the method described above, dual-pairing compatibility trials were then performed, with one 5 mm plug per isolate transferred to each 9 cm diam. Petri dish (seven replicates). Self-by-self pairings were also performed as experimental controls. Observations were made every 3–4 d for 21 d, and vegetative compatibility was then evaluated as described above.

Pathogenicity and compatibility of two diverging monoconidial strains

Tests were performed using the method of Montecchio *et al.* (2015) by placing 3 mm plugs of MC,

MI, MC+MI (vertically joined half plugs) or PDA into stems of ten 3-year-old container-grown *J. nigra* plants per treatment, wounded with a 3 mm diameter cork borer. Inoculation points were protected with Parafilm and the plants maintained in the greenhouse ($21 \pm 2^\circ\text{C}$, 80% relative humidity; 12 h d^{-1} natural light). After 100 d, the resulting necroses were examined, and the area and shape, visible separations between necroses in split-plugged stems, and wound closure status were recorded. Statistical significance was determined by one-way analysis of variance (ANOVA, $P < 0.05$; IBM SPSS Statistics for Windows, Version 22.0, 2013).

Preliminary investigations of mycovirus presence in two monoconidial strains

To investigate the possible presence of a mycovirus in the MC and MI strains, four 1 cm^3 portions were collected from the edges of 10-d-old colonies growing on PDA. As a control, the procedure was replicated with agar from the edges of uncolonized Petri dishes. Samples were homogenized with a mortar and pestle and diluted 1:5 w/v in twice distilled water. The material was subjected to two freezing and thawing cycles at -20°C to break the cell walls and release any viral particles. After centrifugation at $4,500 \times g$ for 20 min (Airfuge[®] A100, Beckman), the supernatant was centrifuged at $10,621 \times g$ for 20 min. Supernatant (0.1 mL) was collected and re-centrifuged at $90,000 \times g$ on formvar-coated copper 200 mesh grids (Electron Microscopy Sciences) and stained with 2% sodium-phosphotungstate (Hayat, 1986; Robards and Wilson, 1993). Observations were performed using a Philips 208 M transmission electron microscope (TEM). Micrographs were recorded using a Gatan charge-coupled device (CCD) camera, and images analyzed using Image Pro Express analytical imaging software (Media Cybernetics).

Results

Preliminary vegetative compatibility tests on naturally infected black and European walnut trees

Throughout the test, isolates 1M, 2M and U mainly grew apart from each other. After 10 d incubation, 1M and 2M isolates contacted, although the mycelia never mingled with U (Figure 3b). Microscope observations between colonies revealed the infrequent presence of hyphal anastomoses in the spac-

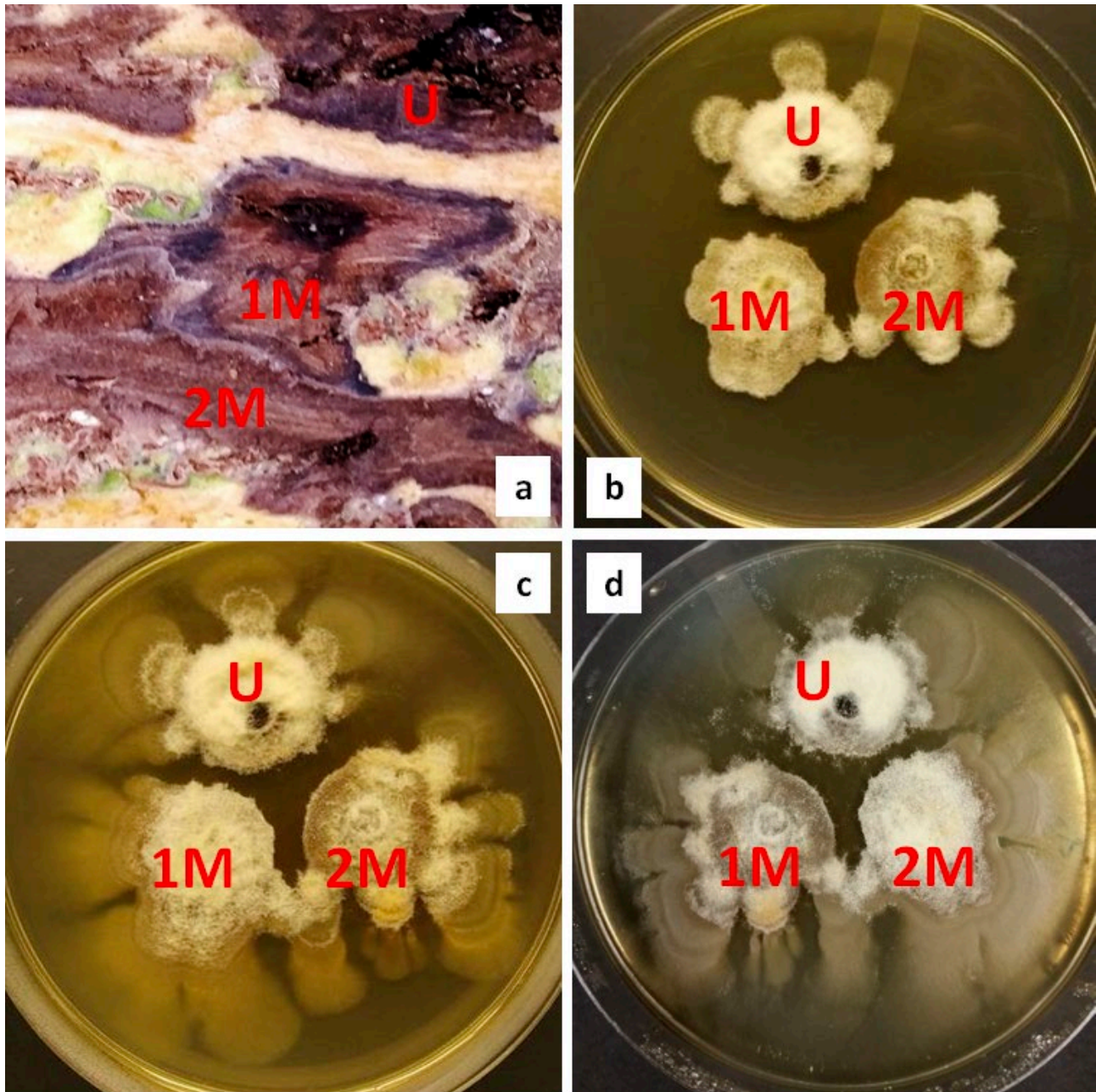


Figure 3. A. Cankers originating from single walnut twig beetle infections on black walnut (previously shown in Figure 2). Partially merging (PM) cankers are separated by a thin discontinuous line (1M and 2M) and unmerging cankers (U) are separated by a wider sub-parallel area. b, c and d: Pairing of the three isolates after 10 d (a) , 30 d (b) and 90 d (c).

es between 1M and 2M isolates, although the true origin of the structures was highly uncertain and self-self anastomoses could not be excluded. After 30 d, merging points between 1M and 2M isolates

increased, confirming the presence of anastomoses between the isolates; the origin of the anastomoses, however, remained uncertain. Isolate 1U never merged with other isolates except for its youngest

portion, growing along the edge of the Petri dish in a narrow space and therefore overlapping 1M and 2M (Figure 3c). Between the U and two M strains, the mycelia showed clear separation. The same behaviour was observed 90 d after inoculation, where the collapse of aerial mycelium adjacent to the gap reaction was sometimes observed (Figure 3d).

Vegetative compatibility between 1M and 2M isolates was categorized as LC, and between U and 1M and 2M as I.

During the test, the self-self-triple control cultures showed full compatibility with viable anastomoses.

Vegetative compatibility in the Italian disease outbreak

Isolate collection, macroscopic categorization and vegetative compatibility among isolates

Codes, geographic origins and macroscopic categorization of the 13 isolated strains of *G. morbida* are reported in Table 1.

Table 1. Isolate code, site and macroscopic features for the 13 *Geosmithia morbida* isolates. Province: VI = Vicenza, TV = Treviso. Pigmentation: W = whitish-orange, and B = orange-brown. Edge shape: E = mainly even and R = mainly rough. Growth rate: F = fast and S = slow. Geographic locations of the isolates are reported in Figure 2.

Isolate	Town, province, plantation code	Pigmentation, edges shape, growth rate
1	Bressanvido, VI, a	W, E, F
2	Bressanvido, VI, b	W, E, S
3	Sandriago VI, a	W, R, F
4	Sandriago, VI, b	W, E, S
5	Dueville, VI, a	W, E, F
6	Dueville, VI, b	B, R, S
7	Thiene, VI, a	B, R, S
8	Thiene, VI, b	W, E, F
9	Schio, VI, a	W, E, F
10	Schio VI, b	W, R, S
11	Schio, VI, c	W, E, F
12	Castelfranco, TV, a	W, E, F
13	Postioma, TV, a	W, R, F

After 21 d of incubation, six isolates (1, 5, 8, 9, 11, and 12) showed whitish-orange pigmentation, even edges and fast growth. Two isolates (6 and 7) were orange-brown, rough edged and slow growing. The remaining isolates showed intermediate features (Figure 4), and merging was frequently observed among pale, even edged, fast-growing colonies.

Microscope observations revealed the presence of hyphal anastomoses between all the FM isolate pairs, and their absence between U pairs. In the PM isolates, the presence of anastomoses was observed but the hyphal origin was uncertain; these interactions were given preliminary classification as LC pairs. The ability to merge and presence of anastomoses were used to identify three vegetative compatibility groups: C, LC and I. All self-self-comparisons demonstrated full compatibility, and as a result, barrage reactions between pairs were not observed. Except for the self-

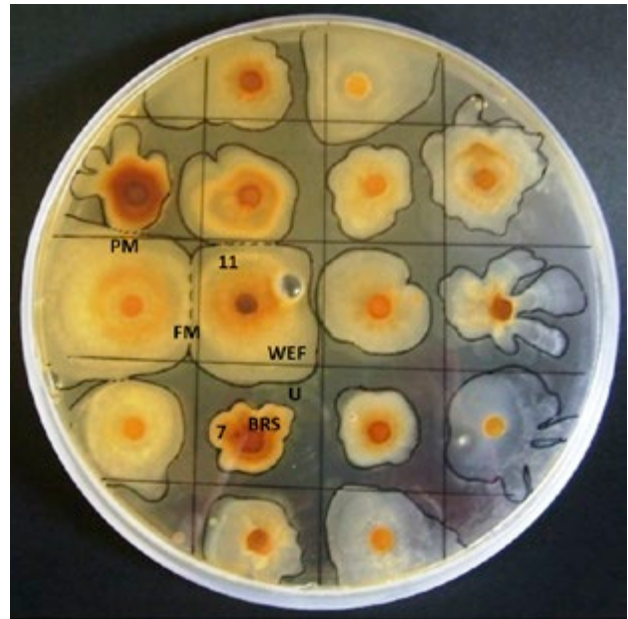


Figure 4. Pigmentation, shape, growth rate, and merging among *Geosmithia morbida* isolates 21 d after incubation. W, whitish-orange; B, orange-brown; E, mainly even; R, mainly rough; F, fast, average diameter ≥ 3 cm; S, slow, average diameter < 3 cm; FM, fully merging, contact ≥ 4 mm; PM, partially merging, contact < 4 mm; U, unmerging, no contact. Isolates 7 and 11 are representatives used to obtain monoconidial strains. Black lines along the colony perimeters on the plate back were used for growth comparisons between the observation dates.

self pairings, incompatibility was observed in 56% of the pairings, with maximum values observed in pairings involving isolate 7 (10/12). Compatibility occurred in 21% of pairings, with maximum values of 5/12 observed for isolates 2 and 11. Uncertain compatibility (LC) was found in 23% of pairings, whereas all self-self pairings demonstrated full compatibility.

Strains 7 and 11 were incompatible and presented opposite compatibility behaviour; strain 7 demonstrated the highest I (10) among the strains with the lowest C (1), whereas strain 11 displayed the lowest I (6) among the colonies with the highest C records (5). Therefore, strains 7 was considered the most representative I isolate, and 11 the most representative C isolate, and were selected to obtain the MI and MC strains.

Table 2 outlines the vegetative compatibility among all combinations of the 13 isolates, which also included self-self-pairings.

In vitro vegetative compatibility between two diverging monoconidial strains

MI and MC monoconidial isolates mirrored the main features observed in the parental isolates, including MI, which were brown, slow growing with rough edges, and MC, which were pale, even edged and fast growing (Figure 5a and b). Incompatibility was observed in every replicate, characterized by a visible separation of at least 3 mm and absence of barrage reactions (Figure 5c) and anastomoses. Self-self pairings showed full compatibility in all replicates and presented viable anastomoses.

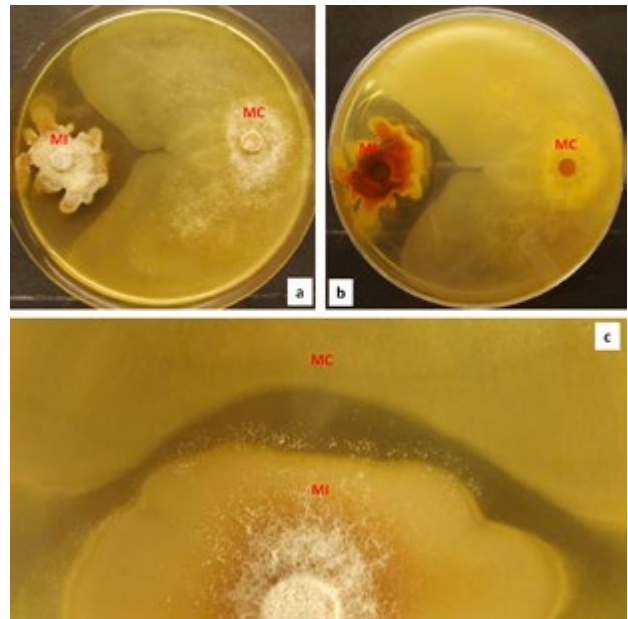


Figure 5. Compatibility trial 21 d after inoculation of *Juglans regia* with *Geosmithia morbida* monoconidial isolates MC and MI obtained from isolate 11 (representative of the compatible strains) and isolate 7 (representative of the incompatible strains). a, front plate; b, reverse; c, detail of a.

Pathogenicity and compatibility between divergent monoconidial strains

One hundred days after inoculation, plants treated with MC, MI and PDA developed nearly even-edged oblong necroses, whereas the plants inocu-

Table 2. Vegetative compatibility among the 13 *Geosmithia morbida* isolates. Red= incompatible (I); yellow = likely compatible (LC); green = compatible (C).

	1	2	3	4	5	6	7	8	9	10	11	12	13
13	Yellow	Red	Green	Yellow	Yellow	Red	Red	Green	Yellow	Yellow	Red	Red	Green
12	Green	Green	Yellow	Yellow	Red	Red	Red	Yellow	Red	Yellow	Green	Green	Green
11	Yellow	Green	Red	Red	Green	Red	Red	Green	Green	Red	Green		
10	Red	Red	Yellow	Red	Red	Green	Red	Red	Yellow	Green			
9	Red	Green	Red	Yellow	Red	Red	Red	Yellow	Green				
8	Yellow	Red	Green	Red	Red	Red	Red	Green					
7	Yellow	Green	Red	Red	Red	Red	Green						
6	Red	Red	Red	Red	Green	Green							
5	Red	Red	Red	Green	Green								
4	Yellow	Green	Yellow	Green									
3	Red	Red	Green										
2	Red	Green											
1	Green												



MC MI MC+MI C

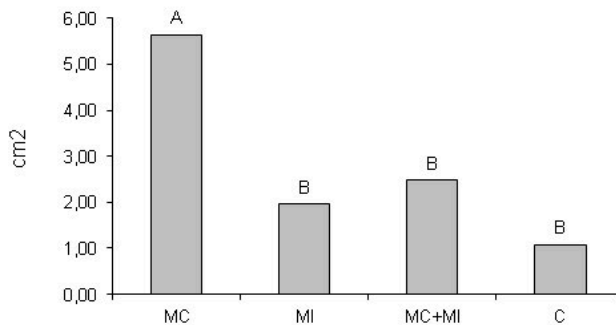


Figure 6. Pathogenicity and compatibility between *Geosmithia morbida* monoconidials 100 d after inoculation. MC, compatible monoconidial; MI, incompatible monoconidial; MC+MI, both monoconidials vertically inoculated (two half-plugs); C, PDA controls. ANOVA, $P < 0.05$.

lated with vertically joined half plugs of MC + MI showed uneven and vertically necroses. MC-treated plants showed a significantly greater necrotic area (average = 5.6 cm²) than MI (1.9 cm²), MC + MI (2.4 cm²) and control plants (1.0 cm²). MC-treated plants also lacked wound closure reactions (Figure 6).

Preliminary investigations of mycovirus presence in the two monoconidial strains

TEM observations of centrifuged samples from the MI isolate revealed many isometric, icosahedral virus-like particles approximately 28–30 nm in diameter (Figure 7). Particles with these characteristics were never observed in extracts from the MC isolate

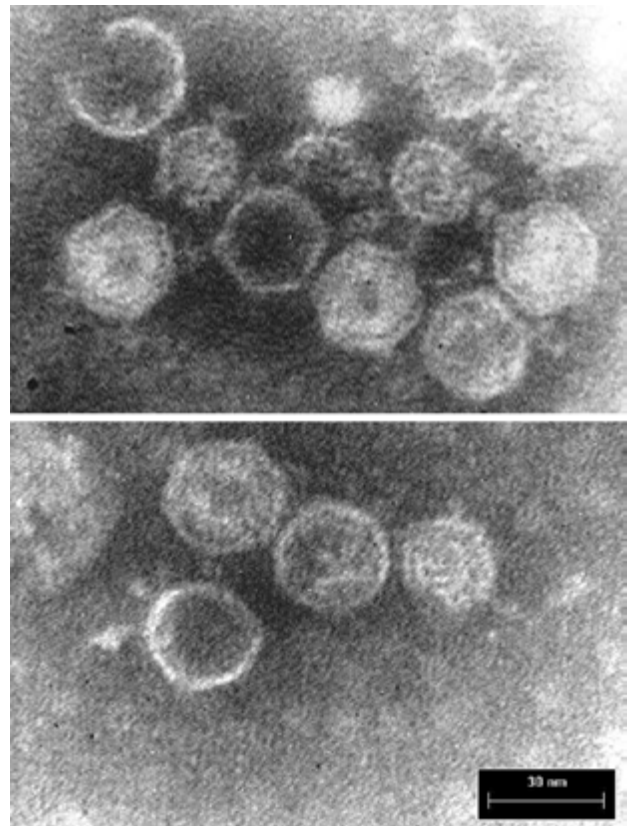


Figure 7. Icosahedral virus-like particles with diameters of approximately 28 nm and observed only in MI samples.

or in the controls. Further observations were not performed.

Discussion

Results from preliminary trials performed on freshly collected, infected black walnut samples demonstrated that mycelia isolated from visibly non-coalescing cankers separated by sub-parallel and unmerging zones may represent incompatibility or low vegetative compatibility within (at least) the Italian population of *G. morbida*. This suggests a likely cause-effect relationship between unmerging cankers and incompatibility reactions among isolates. Several *G. morbida* strains and haplotypes may be present on the same tree (Kolarik *et al.*, 2011; Freeland *et al.*, 2012; Zerillo *et al.*, 2014). According to published reports, the “demarcation reactions” (also called “gap reactions,” “clear zones,” or “line-gaps”;

Brasier, 1986; Schafer and Kohn, 2006; Gross *et al.*, 2012, 2014; Brasier and Webber, 2013) observed between incompatible mycelia can be associated with sub-parallel equidistant pale zones that occur between parental unmerging cankers (Figure 3a), thus delimiting different genotypes of *G. morbida*.

Assuming that the demarcations are antagonistic reactions, the presence of multiple (“thousands”) of neighbouring cankers on the same tree can be attributed to the compulsory feeding behaviour and reproductive strategy of infected vectors (*P. juglandis*, WTB; Tisserat *et al.*, 2009; Zerillo *et al.*, 2014). Furthermore, these non-coalescing infection sites are likely to derive from incompatibility reactions between the mycelia that produce the cankers and competitive establishment of resource domains for the genets in adjacent cankers.

Additional detailed *in vitro* studies on the 13 strains obtained from black walnuts in the Italian outbreak confirmed differences among colonies in pigmentation, shape, and growth rate. The highest frequency of merging was observed between whitish, even-edged, fast-growing colonies. Full vegetative incompatibility (unmerging colonies lacking anastomoses) was observed in 56% of events, and one isolate was compatible with only one different strain.

Despite the use of fresh isolates, mycelial barrage formation between incompatible strains, a typical incompatibility reaction in many Ascomycetes (i.e., *Cryphonectria parasitica* and *Ophiostoma novo-ulmi*; Anagnostakis, 1982; Brasier, 1984, 1986; Brasier and Kirk, 2000; Cortesi and Milgroom, 1998; Smith *et al.*, 2006), was never observed under our experimental conditions. Simple equidistant demarcation reactions without anastomoses were the most consistent features associated with incompatibility (Figure 4, U), suggesting the involvement of enzymes or metabolites (Andersson *et al.*, 2012; Grad *et al.*, 2009) inhibiting the growth of at least one of the two mycelia. This hypothesis is supported by the pairings between monoconidial isolates obtained from the most and least compatible isolates. These revealed large differences in colony features and growth rates, and confirmed previously observed incompatibilities in the parental isolates represented by a wide separation lacking anastomoses and barrage reactions (Figure 5c).

Vegetative incompatibility between strains of the same species that prevents heterokaryon formation

and reduces the spread of cytoplasmic elements that promote outcrossing is a well-known phenomenon in a number of Ascomycetes (Biella *et al.*, 2002; Glass and Demethon, 2006; Smith *et al.*, 2006; Brasier and Webber, 2013). This has obvious ecological and epidemiological consequences. For instance, in *C. parasitica*, which causes chestnut blight, incompatibility between strains colonizing the same tree limits the spread of RNA viruses responsible for canker remission (Nuss, 1992; Cortesi *et al.*, 2001; Smith *et al.*, 2006).

Icosahedral, isometric, 28–30 nm particles, very similar to mycovirus (Buck, 1984; Castro *et al.*, 1999), were observed in one strain of *G. morbida* (MI), characterized by significantly lower pathogenicity than a particles-free (MC) isolate. Visible demarcation reactions between the two incompatible strains appeared when they were simultaneously inoculated. Further investigations of the physical and chemical nature of the demarcation reactions associated with incompatibility are in progress. An additional question is, what is the nature and potential translocation pathways of the virus-like particle? This must be answered to verify if these particles play direct (i.e. hyphal degeneration) or indirect (i.e. stimulating the expression of enzymes or metabolites involved in demarcation reactions) roles in the phenotypic expression of fungal virulence. Under such conditions, the presence of a mycovirus, when confirmed, could be a useful marker for monitoring the structure and dynamics of *G. morbida* populations (Brasier and Kirk, 2000; Liu and Milgroom, 2007; Brasier and Webber, 2013).

Acknowledgements

This research was financially supported by the Regione del Veneto (Resolution 2878/2013) and the University of Padova (ex 60%, 2014). For their cooperation and support, the authors thank G. Zanini and M. Vettorazzo (Regione del Veneto, Servizio Fitosanitario), F. Montesi (Istituto Zooprofilattico Sperimentale delle Venezie), S. Zanella, N. Fassina and L. Cemolin (University of Padova).

This paper is dedicated to Dr. Linda Scattolin, a friend and colleague, who passed away too soon.

Literature cited

Anagnostakis S.L., 1982. Biological control of chestnut blight. *Science* 215, 466–471.

- Andersson P.F., S. Bengtsson, J. Stenlid, A. Broberg, 2012. B-norsteroids from *Hymenoscyphus pseudoalbidus*. *Molecules* 17, 7769–7781.
- Biella S., M.L. Smith, J.R. Aist, P. Cortesi, M.G. Milgroom, 2002. Programmed cell death correlates with virus transmission in a filamentous fungus. *Proceedings of the Royal Society of London - Series B* 269, 2269–2276.
- Brasier C.M., 1984. Inter-mycelial recognition systems in *Ceratocystis ulmi*: their physiological properties and ecological importance. In: *The Ecology and Physiology of the Fungal Mycelium*. (D. Jennings, A.M.D. Rayner, ed.), Cambridge University Press, Cambridge, UK, 451–497.
- Brasier C.M., 1986. The population biology of Dutch elm disease: its principal features and some implications for other host pathogen systems. *Advances in Plant Pathology* 5, 55–118.
- Brasier C.M., 1988. Rapid changes in genetic structure of epidemic populations of *Ophiostoma ulmi*. *Nature* 332, 538–541.
- Brasier C.M., S.A. Kirk, 2000. Survival of clones of NAN *Ophiostoma novo-ulmi* around its probable centre of appearance in North America. *Mycological Research* 104, 1322–1332.
- Brasier C., J. Webber, 2013. Vegetative incompatibility in the ash dieback pathogen *Hymenoscyphus pseudoalbidus* and its ecological implications. *Fungal Ecology* 6, 501–512.
- Buck K.W., 1984. A new double-stranded RNA virus from *Gaeumannomyces graminis*. *Journal of General Virology* 65, 987–990.
- Castro M., Kramer K., Valdivia L., Ortiz S., Benavente J., Castillo A., 1999. A new double-stranded RNA mycovirus from *Botrytis cinerea*. *FEMS Microbiology Letters* 175, 95–99.
- Causin R., G. Frigimelica, L. Montecchio, S. Mutto Accordi, 1995. Vegetative compatibility and conversion to hypovirulence among Italian isolates of *Cryphonectria parasitica*. *European Journal of Forest Pathology* 25, 232–239.
- Cortesi P., M.G. Milgroom, 1998. Genetics of vegetative incompatibility in *Cryphonectria parasitica*. *Applied Environmental Microbiology* 64, 2988–2994.
- Cortesi P., C.E. McCulloch, H. Song, H. Lin, M.G. Milgroom, 2001. Genetic control of horizontal virus transmission in the chestnut blight fungus, *Cryphonectria parasitica*. *Genetics* 159, 107–118.
- Deng F., R. Xu, G. Boland, 2003. Hypovirulence-associated double-stranded RNA from *Sclerotinia homoeocarpa* is conspecific with *Ophiostoma novo-ulmi* mitovirus 3a-Ld. *Phytopathology* 93, 1407–1414.
- Freeland E, W. Cranshaw, N. Tisserat, 2012. Effect of *Geosmithia morbida* isolate and temperature on canker development in black walnut. Online. *Plant Health Progress*. doi: 10.1094/PHP-2012-0618-01-RS.
- Glass N.L., K. Demethon, 2006. Non-self recognition and programmed cell death in filamentous fungi. *Current Opinion in Microbiology* 9, 553–558.
- Grad B., T. Kowalski, W. Kraj, 2009. Studies on the secondary metabolite produced by *Chalara fraxinea* and its phytotoxic influence on *Fraxinus excelsior*. *Phytopathologia* 54, 61–69.
- Gross A., P.L. Zaffarano, A. Duo, C.R. Grúnig, 2012. Reproductive mode and life cycle of the ash dieback pathogen *Hymenoscyphus pseudoalbidus*. *Fungal Genetics and Biology* 49, 977–986.
- Gross A., O. Holdenrieder, M. Pautasso, V. Queloz, T.N. Sieber, 2014. *Hymenoscyphus pseudoalbidus*, the causal agent of European ash dieback. *Molecular Plant Pathology* 15, 5–21.
- Hayat M.A., 1986. *Basic techniques for Transmission Electron Microscopy*. Academic Press Inc., San Diego, CA, USA, 411 pp.
- Hong Y.G., S.L. Dover, T.E. Cole, C.M. Brasier, K.W. Buck, 1999. Multiple mitochondrial viruses in an isolate of the Dutch elm disease fungus *Ophiostoma novo-ulmi*. *Virology* 258, 118–127.
- Kolařík M, E. Freeland, C. Utley, N. Tisserat, 2011. *Geosmithia morbida* sp. nov., a new phytopathogenic species living in symbiosis with the walnut twig beetle (*Pityophthorus juglandis*) on *Juglans* in USA. *Mycologia* 103, 325–332.
- Liu Y.C., M.G. Milgroom, 2007. High diversity of vegetative compatibility types in *Cryphonectria parasitica* in Japan and China. *Mycologia* 99, 279–284.
- Montecchio L., M. Faccoli, 2014. First Record of Thousand Cankers Disease *Geosmithia morbida* and Walnut Twig Beetle *Pityophthorus juglandis* on *Juglans nigra* in Europe. *Plant Disease* 98, 696.
- Montecchio L., G. Fanchin, M. Simonato, M. Faccoli, 2014. First record of Thousand Cankers Disease fungal pathogen *Geosmithia morbida* and Walnut Twig Beetle *Pityophthorus juglandis* on *Juglans regia* in Europe. *Plant Disease* 98, 1445.
- Montecchio L., M. Faccoli, D. Short, G. Fanchin, D. Geiser, M.T. Kasson, 2015. First Report of *Fusarium solani* phylogenetic species 25 associated with early stages of Thousand Cankers Disease on *Juglans nigra* and *Juglans regia* in Italy. *Plant Disease* 99, 1183.
- Nuss D.L., 1992. Biological control of chestnut blight: an example of virus-mediated attenuation of fungal pathogenesis. *Microbiology Review* 56, 561–576.
- Polashock J., P. Bedker, B. Hillman, 1997. Movement of a small mitochondrial double-stranded RNA element of *Cryphonectria parasitica*: ascospore inheritance and implications for mitochondrial recombination. *Molecular and General Genetics* 256, 566–571.
- Regione del Veneto, 2014. *Bollettino ufficiale*. XLV, 83, 26 agosto 2014.
- Robards A.W., A.J. Wilson (ed.), 1993. *Procedures in Electron Microscopy*. Wiley, Chichester UK, 700 pp.
- Rodriguez-Garcia C., V. Medina, A. Alonso, M. Ayllon, 2014. Mycoviruses of *Botrytis cinerea* isolates from different hosts. *Annales of Applied Biology* 164, 46–61.
- Schafer M.R., L.M. Kohn, 2006. An optimized method for mycelia compatibility testing in *Sclerotinia sclerotiorum*. *Mycologia* 98, 593–597.
- Schoebel C. N., S. Zoller, D. Rigling, 2014. Detection and genetic characterisation of a novel mycovirus in *Hymenoscyphus fraxineus*, the causal agent of ash dieback. *Infection, Genetics and Evolution* 28, 78–86.
- Serdani M, J.J. Vlach, K.L. Wallis, M. Zerillo, T. McCleary, N.A. Tisserat, 2013. First report of *Geosmithia morbida* and *Pityophthorus juglandis* causing thousand cankers disease in butternut. Online. *Plant Health Progress*. doi: 10.1094/PHP-2013-1018-01-BR.
- Seybold S.J., T.W. Coleman, P.L. Dallara, N.L. Dart, A.D. Graves, L.A. Pederson, S.E. Spichiger, 2012. Recent collect-

- ing reveals new state records and geographic extremes in the distribution of the walnut twig beetle, *Pityophthorus juglandis* Blackman (Coleoptera: Scolytidae) in the United States. *Pan-Pacific Entomologist* 88, 277–280.
- Smith M.L., C.C. Gibbs, M.G. Milgroom, 2006. Heterokaryon incompatibility function of barrage-associated vegetative incompatibility genes (vic) in *Cryphonectria parasitica*. *Mycologia* 98, 43–50.
- Tisserat N., W. Cranshaw, D. Leatherman, C. Utley, K. Alexander, 2009. Black walnut mortality in Colorado caused by the walnut twig beetle and thousand cankers disease. Online. *Plant Health Progress*. doi: 10.1094/PHP-2009-0811-01-RS.
- Tisserat N., W. Cranshaw, M.L. Putnam, J. Pscheidt, C.A. Leslie, M. Murray, J. Hoffman, Y. Barkley, K. Alexander, S.J. Seybold, 2011. Thousand cankers disease is widespread in black walnut in the western United States. Online. *Plant Health Progress*. doi: 10.1094/PHP-2011-0630-01-BR.
- Utley C., T. Nguyen, T. Roubtsova, M. Coggeshall, T.M. Ford, L.J. Grauke, A.D. Graves, C.A. Leslie, J. McKenna, K. Woeste, M.A. Yagmour, W. Cranshaw, S.J. Seybold, R.M. Bostock, N. Tisserat, 2013. Susceptibility of walnut and hickory species to *Geosmithia morbida*. *Plant Disease* 97, 601–607.
- Wood S.L., D.E. Bright, 1993. *A Catalog of Scolytidae and Platypodidae (Coleoptera), Part 2: Taxonomic Index*. Great Basin Naturalist Memoirs 13, Brigham Young University, UT, USA, 1553 pp.
- Wu M., L. Zhang, G. Li, D. Jiang, M. Hou, H.C. Huang, 2007. Hypovirulence and double-stranded RNA in *Botrytis cinerea*. *Phytopathology* 97, 1590–1599.
- Zerillo M.M., J. Ibarra Caballero, K. Woeste, A.D. Graves, C. Hartel, J.W. Pscheidt, J. Tonos, K. Broders, W. Cranshaw, S.J. Seybold, N. Tisserat, 2014. Population Structure of *Geosmithia morbida*, the Causal Agent of Thousand Cankers Disease of Walnut Trees in the United States. *PLoS ONE* 9(11): e112847. doi: 10.1371/journal.pone.0112847.
- Zhou T., G.J. Boland, 1997. Hypovirulence and double-stranded RNA in *Sclerotinia homoeocarpa*. *Phytopathology* 87, 147–153.

Accepted for publication: July 1, 2015

Published online: October 7, 2015